Weak-Field Galvanomagnetic Properties of a New Type of Metallic Model*

R. S. Allgaier
U.S. *Naval Ordnance Laboratory, Silver Spring, Maryland* 20910

and

Robert Perl
U.S. *Naval Ordnance Laboratory, Silver Spring, Maryland* 20910
and University of Maryland, College Park, Maryland 20742

(Received 2 March 1970)

The weak-field Hall coefficient and magnetoresistance are computed for a metallic model in which the Fermi surface has the form of a cube with rounded edges and corners. Exact and relatively simple results are obtained as a function of a parameter which allows the shape of the Fermi surface to evolve continuously from a sphere to a cube with sharp edges and corners. In going from the one extreme to the other, the Hall coefficient decreases monotonically from $1/ne$ to $\frac{1}{4}\pi/ne$, while the Seitz magnetoresistance coefficients b, c, and d increase monotonically from zero to infinity (for b and d) and to $1-(8/3\pi)$ (for c). The results are interpreted and compared with the galvanomagnetic properties of other types of models.

I. INTRODUCTION

This paper presents a calculation of the weak-field Hall coefficient and the Seitz weak-field magnetoresistance coefficients for a new type of cubically symmetric model. The calculation is exact and relatively simple, even though the model assumes a Fermi surface which becomes highly distorted for certain values of a shape parameter.

The paper is the result of a search for a simple way to compute magnetoresistance in anisotropic nonellipsoidal models. Except when the Fermi surface is spherical or ellipsoidal, magnetoresistance calculations are generally so complicated that it is impossible to understand the connection between what went into the calculation and what came out. The goal of the present work is to throw some light on that connection.

A very simple technique was developed in an earlier paper for computing the weak-field Hall coefficient in metallic models.[1,2] The essense of the method is to replace the actual Fermi surface by one composed entirely of planar faces intersecting in sharp edges. But this kind of model cannot be used to calculate weak-field magnetoresistance; the effect turns out to be linear, not quadratic, in the magnetic field,[3,4] and hence, it is not a true weak-field magnetoresistance.

In the present work we get around this difficulty by rounding the edges and corners at which the planar faces meet. The calculation does not become complicated because the Fermi surface is constructed from a combination of simple shapes: planes, cylinders, and spheres.

II. MODEL

A sketch of the Fermi surface used in the calculation is presented in Fig. 1. It is a cube from which the sharp edges and corners have been removed by rounding them off into cylindrical and spherical forms, respectively. Opposite flat faces are separated by the distance $2p_f$. The radius of the cylindrical and spherical portions is sp_f. Thus, the length of the edges of the flat faces is $2 \times (1-s)p_f$. As $s \to 1$, the flat and cylindrical faces disappear, and the surface becomes spherical. As $s \to 0$, the surface becomes a cube with sharp

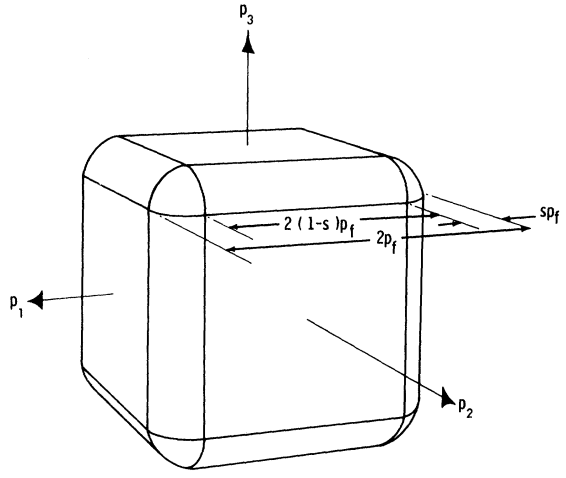

FIG. 1. Fermi-surface model used in the calculation (see Sec. II).

edges.

At first we assumed that $s \ll 1$ (i.e., the rounded portions constituted a very small fraction of the total surface area) because we were interested in determining the magnetoresistance in a model which resembled as closely as possible the planar-faced sharp-edged models used in the Hall coefficient work.[1,2] But it turned out that exact results were easily obtainable for any fraction of curved surface. Thus, it was possible to study the evolution of the magnetoresistance coefficients as the Fermi surface deforms from an isotropic to a highly anisotropic form.

To carry out the calculations, however, it was necessary to specify not only the Fermi surface itself but also its evolution in momentum space as a function of energy, i.e., energy-momentum derivatives were required.

One possibility is the constant-shape model shown (in cross section) in Fig. 2(a). As the energy changes from $\mathcal{E}$ to $\mathcal{E}+\Delta\mathcal{E}$, the constant-shape assumption requires that the boundaries between the flat and cylindrical parts of the surface shift from the points q to q', and that the axis of the curved surface shift from point p_0 to p_0'. In this model, the gradient and higher energy-momentum derivatives are very complicated functions on the curved parts of the Fermi surface.

These complications may be avoided by using the model shown in Fig. 2(b). For purposes of differentiation, we assume that the centers of the curved portions of the constant-energy surfaces remain "temporarily" fixed at the point p_0 in momentum space. Now the curves at $\mathcal{E}$ and $\mathcal{E}+\Delta\mathcal{E}$ are separated by a fixed radial distance, and the derivatives on the curved surfaces become much simpler. In particular, the magnitude of the gradient $\vec{v}=\vec{\nabla}_p\mathcal{E}$ is constant, and is equal to its value on the flat faces.

This artifice does not affect the results significantly, since the difference between the positions of the curves at $\mathcal{E}+\Delta\mathcal{E}$ in Figs. 2(a) and 2(b) is small at all points compared to the separation of either curve from the curve at $\mathcal{E}$.

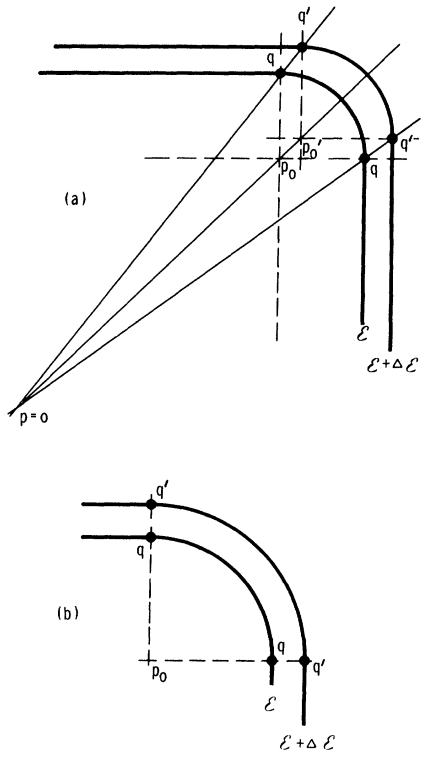

FIG. 2. Two alternatives for the evolution of the Fermi surface as a function of energy $\mathcal{E}$.

III. CALCULATION AND RESULTS

The Fermi surface shown in Fig. 1 is centered on the origin of an orthogonal coordinate system in momentum space (axes p_1, p_2, and p_3) which coincides with the cubic axes of the surface.

The flat faces of the Fermi surface at $\mathcal{E}=\mathcal{E}_F$ lie on the planes $p_i=\pm|p_f|$, $i=1$, 2, and 3. Normal to these faces, we assume the parabolic relation

$$\mathcal{E}=p_i^2/2m\,, \tag{1}$$

where $i=1$, 2, and 3, with m a constant. This is a convenience, not a necessity. Later, we will describe how the final results are altered if the relation

$$g(\mathcal{E})=p_i^2/2m \tag{2}$$

is used instead of Eq. (1); $g(\mathcal{E})$ is a monotonically increasing but otherwise arbitrary function of $\mathcal{E}$.

The axes of the cylindrical parts of the Fermi surface form the edges of a cube with corners at $(\pm|p_0|, \pm|p_0|, \pm|p_0|)$. The faces of this inner cube are separated from the corresponding flat faces of the Fermi surface by the distance $s|p_f|$.

The coordinates of the four cylinder axes parallel to p_3, for example, are $p_{0i}=\pm|p_0|$ $=\pm(1-s)|p_f|$, $i=1$ and 2. The equations of the cylindrical sections centered on these four axes are

$$(p_1-p_{01})^2+(p_2-p_{02})^2=[(2m\mathcal{E})^{1/2}-|p_0|]^2\,. \tag{3}$$

Similarly, the eight spherical corners are given by

$$(p_1-p_{01})^2+(p_2-p_{02})^2+(p_3-p_{03})^2 =[(2m\mathcal{E})^{1/2}-|p_0|]^2\,. \tag{4}$$

The various derivatives needed are obtained from Eqs. (1), (3), and (4), keeping in mind that p_0 is to be regarded as a constant. The nonzero compo-

nent of $\vec{\nabla}_p \mathcal{E}$ on the flat faces perpendicular to p_i is

$$v_i = \pm |p_f|/m \tag{5}$$

at $\mathcal{E} = \mathcal{E}_F$, with $i = 1$, 2, or 3. On the cylindrical and spherical surfaces, we have

$$v_i = \left\{ \frac{p_i - p_{0i}}{[(2m\mathcal{E})^{1/2} - |p_0|]} \left(\frac{2\mathcal{E}}{m}\right)^{1/2} \right\}_{\mathcal{E} = \mathcal{E}_F}$$

$$= \frac{p_i - p_{0i}}{|p_f| - |p_0|} \frac{|p_f|}{m} , \tag{6}$$

where $i = 1$, 2, or 3, but the component parallel to each cylinder axis is excluded. Both Eqs. (5) and (6) may be written in the compact form

$$v_i = \alpha_i (|p_f|/m) , \tag{7}$$

where α_i is the direction cosine of $\vec{v}$ with respect to the ith axis.

The second derivatives (i.e., the components of the reciprocal effective-mass tensor) are

$$\left(\frac{1}{m}\right)_{ij} \equiv \frac{\partial^2 \mathcal{E}}{\partial p_i \partial p_j} = \frac{1}{sm} [\delta_{ij} - (1-s)\alpha_i \alpha_j], \tag{8}$$

where δ_{ij} is the Kronecker δ. The indices i and $j = 1$, 2, or 3, but exclude those values for which α_i or α_j is zero. When $s \ll 1$, $(1/m)_{ij}$ becomes a very anisotropic tensor. This corresponds to the fact that the carriers have an effective mass m when they move in the normal direction to any part of the Fermi surface, but an effective mass sm when they move *along* the curved part of the Fermi surface. To put it another way, the angular velocity of the carriers moving on the curved surface is $1/s$ times larger than it would have been on a spherical Fermi surface of radius p_f.

Another distinctive feature of the model is the appearance of nonzero third derivatives. All of them have the form

$$\frac{\partial^3 \mathcal{E}}{\partial p_i \partial p_j \partial p_k} = -\frac{1}{s^2 |p_f| m} \times (\delta_{ij}\alpha_k + \delta_{jk}\alpha_i + \delta_{ki}\alpha_j - 3\alpha_i \alpha_j \alpha_k) . \tag{9}$$

Again, i, j, and $k = 1$, 2, or 3, but exclude values for which α_i, α_j, or $\alpha_k = 0$. Note that Eq. (9) is nonzero only on the curved parts of the Fermi surface.

We next substitute Eqs. (7)–(9) into the standard expressions which constitute the Jones-Zener weak-field solution to the Boltzmann equation.[5] Degenerate statistics and an isotropic scattering time τ are assumed. It is important to note that use of the standard weak-field solution implies that carriers on the curved parts of the Fermi surface turn through a small angle during the time τ, no matter how sharp the curves may become. If the relation between the current density $\vec{I}$, the electric field $\vec{E}$, and the magnetic field $\vec{H}$ is written

$$I_i = \sigma_{ij} E_j + \sigma_{ijk} E_j H_k + \sigma_{ijkl} E_j H_k H_l + \cdots , \tag{10}$$

the results may be expressed as three types of integrals over the Fermi surface S_F:

$$\sigma_{ij} = \left(\frac{2}{h^3}\right) \frac{e^2 \tau |p_f|}{m} \int_{S_F} \alpha_i \alpha_j \, dS_F , \tag{11}$$

$$\sigma_{ijk} = \left(\frac{2}{h^3}\right) \frac{e^3 \tau^2 |p_f|}{m} \int_{S_F} \alpha_i \alpha_r \left(\frac{1}{m}\right)_{sj} \epsilon_{krs} \, dS_F , \tag{12}$$

and

$$\sigma_{ijkl} = \left(\frac{2}{h^3}\right) \frac{e^4 \tau^3 |p_f|}{m} \int_{S_F} \alpha_i \alpha_t \left[\left(\frac{1}{m}\right)_{ur} \left(\frac{1}{m}\right)_{sj} + \frac{|p_f|}{m} \alpha_r \frac{\partial^3 \mathcal{E}}{\partial p_u \partial p_s \partial p_j} \right] \epsilon_{ltu} \epsilon_{krs} \, dS_F , \tag{13}$$

where h is Planck's constant, e is the carrier charge, and ϵ_{abc} is the permutation tensor. Summation over repeated indices (r, s, t, u) is implied in Eqs. (10)–(13) and wherever else they appear in the equations to follow.

The final form of the results becomes much simpler by using the relation between carrier density and the volume in momentum space enclosed by the Fermi surface:

$$n = (2/h^3)(2|p_f|)^3 [1 - (3 - \tfrac{3}{4}\pi) s^2 + (2 - \tfrac{7}{12}\pi) s^3] . \tag{14}$$

Then we have

$$\sigma_{ii} \equiv \sigma_0 = \frac{ne^2\tau}{m} \left\{ \frac{1 - (2 - \frac{1}{2}\pi) s + (1 - \frac{1}{3}\pi) s^2}{1 - (3 - \frac{3}{4}\pi) s^2 + (2 - \frac{7}{12}\pi) s^3} \right\}, \tag{15}$$

$$\sigma_{ijk} = \frac{ne^3\tau^2}{m^2} \left\{ \frac{\epsilon_{ijk} (\frac{1}{4}\pi)(1 - \frac{1}{3}s)}{1 - (3 - \frac{3}{4}\pi) s^2 + (2 - \frac{7}{12}\pi) s^3} \right\}, \tag{16}$$

$$\sigma_{iiii} = 0 , \tag{17a}$$

$$\sigma_{iijj} = -\frac{ne^4\tau^3}{m^3} \left\{ \frac{(\pi/4s)(1 - \frac{1}{3}s)}{1 - (3 - \frac{3}{4}\pi) s^2 + (2 - \frac{7}{12}\pi) s^3} \right\}, \tag{17b}$$

$$\sigma_{ijij} = \frac{ne^4\tau^3}{m^3} \left\{ \frac{\frac{1}{6}\pi}{1 - (3 - \frac{3}{4}\pi) s^2 + (2 - \frac{7}{12}\pi) s^3} \right\}, \tag{17c}$$

and $\sigma_{ijji} = 0$, (17d)

where i, j, and k may equal 1, 2, or 3, but must be different from one another. No other classes of terms (e.g., σ_{ij}, σ_{iij}, or σ_{ijki}) can possibly be nonzero for any model with cubic symmetry of types $m3m$, $\bar{4}3m$, or 432.

The weak-field Hall coefficient is given by $R_0 = \sigma_{123}/\sigma_0^2$; therefore,

$$R_0 = (\tfrac{1}{4}\pi/ne) [1 - \tfrac{1}{3}s - (3 - \tfrac{3}{4}\pi) s^2 + (3 - \tfrac{5}{6}\pi) s^3 - (\tfrac{2}{3} - \tfrac{7}{36}\pi) s^4] / [1 - (2 - \tfrac{1}{2}\pi) s + (1 - \tfrac{1}{3}\pi) s^2]^2 . \tag{18}$$

We define a dimensionless weak-field magnetoresistance $M_{\alpha\beta\gamma}{}^{\delta\epsilon\xi}$ by the relation

$$\Delta\rho/\rho_0 = M_{\alpha\beta\gamma}{}^{\delta\epsilon\zeta}(\mu_H H/C)^2, \tag{19}$$

where $\Delta\rho/\rho_0$ is the fractional change in the zero-field resistivity, $\alpha\beta\gamma$ and $\delta\epsilon\zeta$ identify the current and magnetic field directions relative to the cubic axes, $\mu_H (= R_0\sigma_0)$ is the Hall mobility, and C is the compatability factor between the electrical and magnetic units used.

Then the dimensionless Seitz coefficients b, c, and d are related to Eq. (19) by

$$M_{\alpha\beta\gamma}{}^{\delta\epsilon\zeta} = b + c\,(\iota_i\eta_i)^2 + d(\iota_i^2\eta_i^2), \tag{20}$$

where ι_i and η_i are the direction cosines of the current and magnetic field directions in the cubic-axis system.

The relations between the components of Eq. (10) and b, c, and d are

$$b = -D\sigma_{iijj} - 1\,, \tag{21a}$$

$$c = -D(\sigma_{ijij} + \sigma_{ijji}) + 1\,, \tag{21b}$$

and

$$d = -D(\sigma_{iiii} - \sigma_{iijj} - \sigma_{ijij} - \sigma_{ijji}), \tag{21c}$$

where $D = \sigma_0/\sigma_{ijk}^2$. Substituting Eqs. (15)–(17) into Eqs. (21) leads to the final result

$$b = \frac{(4/\pi s)\left[1 - (2 - \frac{1}{2}\pi)\,s + (1 - \frac{1}{3}\pi)\,s^2\right]}{(1 - \frac{1}{3}s)} - 1\,, \tag{22a}$$

$$c = -\frac{(8/3\pi)\left[1 - (2 - \frac{1}{2}\pi)\,s + (1 - \frac{1}{3}\pi)\,s^2\right]}{(1 - \frac{1}{3}s)^2} + 1\,, \tag{22b}$$

and $$d = -(b + c)\,. \tag{22c}$$

The last relation follows immediately from Eqs. (21) and (17a).

Because degenerate statistics and an isotropic τ were assumed, R_0 depends only on n and s, and b, c, and d depend on s alone. Figures 3 and 4 present numerical results for the Hall factor r ($R_0 = r/ne$) and the Seitz coefficients b and c as functions of s.

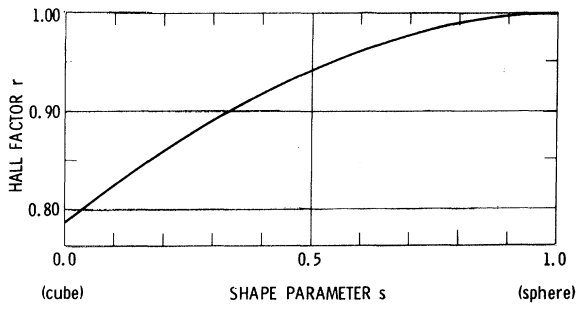

FIG. 3. Graph of the Hall factor r ($R_0 = r/ne$) as a function of the shape parameter s [Eq. (18)].

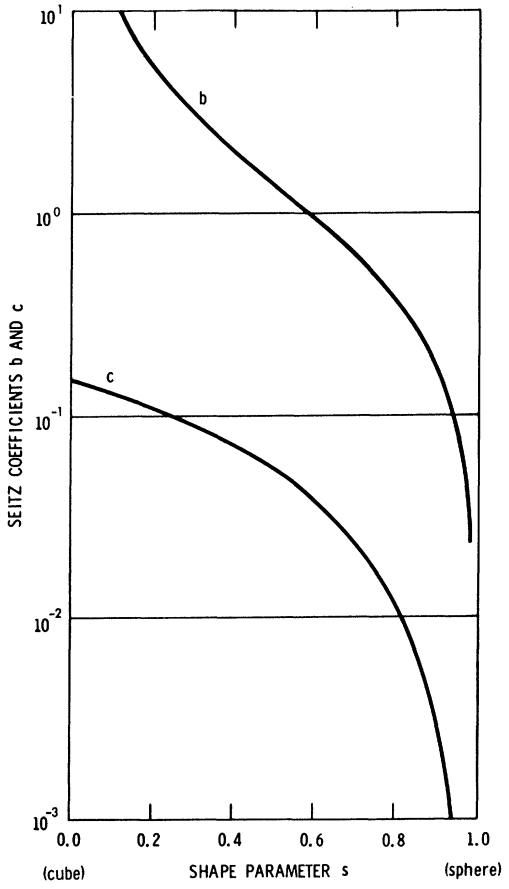

FIG. 4. Graph of the Seitz magnetoresistance coefficients b and c as a function of the shape parameter s [Eqs. (22a) and (22b)].

We have also carried through the calculation without assuming degenerate statistics, and using the nonparabolic relation [Eq. (2)] instead of the parabolic one [Eq. (1)].

Then the second-, third-, and fourth-rank tensors in the expressions for b, c, and d [Eqs. (21)] take on the form

$$\sigma_z = \int \left\{ \frac{\partial[g^{-1}(\mathcal{E})]}{\partial\mathcal{E}} \right\}^{z-1} \tau^{z-1} A_z(\mathcal{E}) \left(\frac{\partial f_0}{\partial\mathcal{E}} \right) d\mathcal{E}\,, \tag{23}$$

where $A_z(\mathcal{E})$ is the function inside the curly brackets in the results for those tensors as given in Eqs. (15)–(17), f_0 is the unperturbed distribution function, and z is the rank of the tensor.

Since the new results for b, c, and d each contain the factor $\sigma_2\sigma_4/\sigma_3^2$, the magnetoresistance symmetry is unaffected; furthermore, the effect of the nonparabolic factor $g(\mathcal{E})$ vanishes when the statistics become degenerate.

IV. DISCUSSION

A. Hall Coefficient

Very little need be said about the behavior of the weak-field Hall coefficient. The Hall factor r starts out at unity for $s=1$, as it should for a spherical Fermi surface. It decreases monotonically with decreasing s, i.e., with increasing distortion, and approaches the value $\frac{1}{4}\pi$ as the Fermi surface approaches the limiting form of a cube with sharp edges [Eq. (19) and Fig. 3].

This behavior is in accord with the rules for the general behavior of the Hall coefficient, i.e., r should drop below unity from shape distortion alone, and it should decrease as the surface becomes more highly distorted.[1,2]

The minimum value of $\frac{1}{4}\pi$ corresponds to the true weak-field limit, as noted in Sec. III and discussed elsewhere.[2] No matter how sharp the edges become, the magnetic field $\vec{H}$ is always assumed to be so small that the Hall angle remains small for carriers moving on the curved parts of the surface. If $\vec{H}$ is kept at a small but fixed value, then ultimately $r\to\frac{1}{2}$. This corresponds to a mixed-field limit in which carriers either stay on one face or go completely around a corner, i.e., the Hall angles are either 0° or 90°.

Since the high-field limit for a closed simply connected Fermi surface is $r=1$, $r(H)$ should go through a minimum value at intermediate $\vec{H}$. This kind of behavior probably accounts for similar characteristics seen in p-type Ge and Si.[6]

B. Magnetoresistance

The model chosen for this paper is potentially useful for understanding the general behavior of weak-field magnetoresistance because it is a metallic single-pocket model which predicts a nonzero effect of considerable magnitude (except when s is close to unity). Consequently, the model corresponds to the situation most commonly encountered in real materials, viz., a substantial magnetoresistance arises because carriers on different parts of the same Fermi surface respond in a significantly different fashion to a given set of applied forces.

This is to be contrasted with the more widely investigated, but more restricted type of model which is realistic only near band edges. Here it is usually assumed that the constant-energy surfaces are spherical or ellipsoidal. But single surfaces of either shape predict a zero magnetoresistance in the metallic approximation. A small or modest effect arises from the energy-dependent response of carriers if the statistics are not degenerate, but this of course restricts the applicability of the model to semiconductors or semimetals.

The only simple band-edge model which predicts a large magnetoresistance is the multivalley model with highly prolate or highly oblate ellipsoidal energy surfaces. But this is still a very special situation in which the effect does not originate within the individual anisotropic surfaces, but is due rather to the different responses of the electrons in differently oriented valleys.

With the above remarks about the nature and applicability of magnetoresistance models in mind, we may now examine the magnetoresistance characteristics of the present model.

In analogy with the rules for the general behavior of the weak-field Hall coefficient,[2] we anticipate that (since τ is isotropic) the magnetoresistance will depend only on the shape of the Fermi surface and how that shape evolves as a function of energy.

Shape evolution enters the problem in a minor way – it is present only because the slightly modified model in Fig. 2(b) was used instead of the constant-shape version shown in Fig. 2(a).

We noted in Sec. III that substituting $g(\mathcal{E})$ for $\mathcal{E}$ had no effect on the results when the statistics are degenerate. This follows because the substitution does not change the shape or the shape-evolution factors at the Fermi energy.

And, in general, only modest changes are to be anticipated when the statistics are not degenerate, because an energy-dependent response is never an important source of magnetoresistance except in the special circumstance that carriers on one energy surface produce little or no effect by themselves.

A magnetoresistance symmetry parameter x may be defined by the relation

$$b+c+xd=0\ . \tag{24}$$

An unanticipated general characteristic of the present magnetoresistance results is that $x=1$ for all values of the shape parameter s. This is to be contrasted with the known result that even a very slight deviation from an isotropic model makes $x\neq 1$.[7]

This condition $x=1$ does occur in a $\langle 100\rangle$-oriented ellipsoidal mullivalley model.[8] At first glance, that does not make the present results more understandable because the cube-shaped Fermi surface may be regarded as an approximation to a spherical surface which has been pulled out along the $\langle 111\rangle$ directions in momentum space. For a $\langle 111\rangle$-oriented ellipsoidal multivalley model $x=0$.[8] But a closer look at the model reveals the origin of the $x=1$ condition, and demonstrates how sensitively the magnetoresistance symmetry depends on the detailed nature of the Fermi-surface distortion.

The model in Fig. 1 may be taken apart and, without rotating any of the pieces, reassembled into a three-band model which is composed of a sphere, three cylinders, and three flat "pancakes."
Each of these bands is equivalent to a ⟨100⟩ ellipsoidal multivalley model. The values of mass ratio K which characterize the anisotropy of the valleys are 1, ∞, and 0 for the sphere, cylinders, and pancakes, respectively.

But the relationship among b, c, and d in a multivalley model is the direct consequence of a corresponding relationship among appropriate components of the magnetoconductivity tensor σ_{ijkl}. Since the contributions to the latter from different bands are additive, it follows that the value of the symmetry parameter x for any number of multivalley bands having a given type of valley orientation is the same as for one set of valleys having that orientation. Hence, in this case, $x=1$.

The other major aspect of the magnetoresistance results that needs to be assessed is the over-all dependence of b, c, and d on the shape of the Fermi surface. For $s=1$, b, c, and d are all zero, as expected for an isotropic metallic model. As the surface deforms, b and d grow, approaching infinity as $s \to 0$, while c never rises above 0.15 or so [Eqs. (22) and Fig. 4].

Because of the nature of Eq. (20) which relates b, c, and d to the experimentally measurable magnetoresistance $M_{\alpha\beta\gamma}{}^{\delta\epsilon\xi}$, all transverse magnetoresistance coefficients increase without limit as $s \to 0$, as do all longitudinal magnetoresistance coefficients except one. The single exception is $M_{100}^{100} (= b + c + d)$. This is identically zero at all values of s because $x=1$.

It is not surprising to discover that the magnetoresistance generally becomes large as the Fermi surface becomes more and more highly distorted. Other examples of the same phenomenon are the cubically symmetric ellipsoidal multivalley models in the highly oblate region.[9] However, there is an important distinction between the two cases. In the multivalley model, the valleys would ultimately intersect one another as they were made more and more oblate, so that this is a rather unrealistic kind of model. In the present case, all values of magnetoresistance between zero and infinity arise from a cube of electronic states of a fixed size simply by rounding off its edges to various degrees.

Another simple model which can lead to a large magnetoresistance is the isotropic two-band model.[10] In weak fields

$$\frac{\Delta\rho}{\rho_0} = \frac{n_1 n_2 \mu_1 \mu_2 (\mu_1 + \mu_2)^2 H^2}{(n_1\mu_1 + n_2\mu_2)^2 C^2}, \tag{25}$$

where n_1 and μ_1, and n_2 and μ_2 are the densities and mobilities of the carriers in bands 1 and 2, respectively. If $(\mu_1 H)^2$ is factored out of the right-hand side of Eq. (25), then we may define a dimensionless magnetoresistance analogous to that given in Eq. (19) as

$$M = tb(1+b)^2/(1+tb)^2, \tag{26}$$

where $t = n_2/n_1$ and $b = \mu_2/\mu_1$.

The term M, given by Eq. (26), can become large. But it pertains to an isotropic two-band model while the present calculation (for $s \ll 1$) was carried out for a highly anisotropic single-band category; therefore, it appears that the two magnetoresistance results become large for quite different reasons. But this is not the case.

We examine Eq. (26) under the circumstance that there are a relatively small number of relatively high-mobility holes in band 2, i.e., $t \ll 1$ and $b \gg 1$. If, in addition, $tb \gg 1$ (this means that most of the conductivity takes place in band 2), then $M \approx b/t$.

The large magnetoresistance results obtained in the present paper (when $s \ll 1$) may be viewed in a similar light. The band-2 characteristics now apply to the carriers on the curved portion of the Fermi surface. Their numbers are relatively small because s is small. Their "magnetoresistance mobility" (i.e., their mobility as they move *along* the curved part of the surface) is relatively high because τ is the same on all parts of the surface, and their mass is sm rather than m. Thus, the sharper the edges become, the higher the carrier mobility becomes there, relative to its value on the flat surfaces, and the larger M becomes.

Finally, we note that the magnitude of c remains small for all values of s. Whether or not this is a general characteristic of a single highly distorted cubically symmetric Fermi surface remains to be seen. It is not a characteristic of the cubically symmetric multivalley models. In the highly oblate limit, b, c, and d all become large.[9]

We know of one possibly pertinent experimental result. In SnTe, a highly degenerate semiconductor, b is as much as six times larger than c.[11] This compound does have a multivalley band structure, but the magnetoresistance symmetry does not correspond to any of the ellipsoidal multivalley models,[8] and theoretical calculations indicate that the valleys have a highly distorted nonellipsoidal shape.[12]

V. CONCLUDING REMARKS

We noted above that the kind of model which makes Hall coefficient calculations so simple cannot be used to calculate weak-field magnetoresis-

tance. What we used here instead – a Fermi surface having flat faces connected by simple types of curved surfaces – did make it possible to carry out a relatively simple computation of the Seitz magnetoresistance coefficients in a highly distorted, nonellipsoidal model. In all probability, no other kind of nonellipsoidal model would have led to a simpler calculation.

However, it will not be as easy to use this kind of model as an approximation to a variety of real Fermi surfaces as it was in the case of the Hall coefficient. But in view of the enormous complexity of most magnetoresistance calculations, we hope that this single example has provided some useful insight into the general behavior of weak-field magnetoresistance.

---

*Work supported in part by ONR Contract No. PO-9-0163.

[1]R. S. Allgaier, Phys. Rev. 165, 775 (1968).
[2]R. S. Allgaier, Phys. Rev. (to be published).
[3]See Ref. 1, note added in manuscript.
[4]H. Miyazawa, in *Proceedings of the International Conference on the Physics of Semiconductors, Exeter* (The Institute of Physics and the Physical Society, London, 1962), p. 636.
[5]A. C. Beer, *Galvanomagnetic Effects in Semiconductors* (Academic, New York, 1963), Chap. 3.
[6]Reference 5, pp. 201–204.
[7]L. Davis, Phys. Rev. 56, 93 (1939).
[8]Reference 5, p. 231.
[9]Reference 5, pp. 231–241.
[10]Reference 5, Chap. VI.
[11]C. C. Evans, T. A. Reglein, and R. S. Allgaier, this issue, Phys. Rev. B 2, 980 (1970).
[12]M. Cohen (private communication).

PHYSICAL REVIEW B VOLUME 2, NUMBER 4 15 AUGUST 1970

Electronic Structure of the fcc Transition Metals Ir, Rh, Pt, and Pd†

O. Krogh Andersen*
Laboratory for Electrophysics, Technical University, Lyngby, Denmark

and

Physics Department, University of Pennsylvania, Philadelphia, Pennsylvania 19104
(Received 11 December 1969)

We give a complete description of a relativistic augmented-plane-wave calculation of the band structures of the paramagnetic fcc transition metals Ir, Rh, Pt, and Pd. The width and position of the d band decrease in the sequence Ir, Pt, Rh, Pd; and $N(E_F) = 13.8$, 23.2, 18.7, and 32.7 (states/atom)/Ry, respectively. Spin-orbit coupling is important for all four metals and the coupling parameter varies by 30% over the d bandwidth. Detailed comparisons with de Haas–van Alphen Fermi-surface dimensions have previously been presented and the agreement was very good. Comparison with measured electronic specific-heat coefficients γ and cyclotron masses indicate that the average mass enhancements are 1.37, 1.44, 1.63, and 1.66 for Ir, Rh, Pt, and Pd, respectively; and that for both Pt and Pd the partial enhancements on the closed electron surface and on the open hole surface are 1.51 and 1.68, respectively. Saddle points in the fifth band are important for the large peak in $N(E)$ near the top of the d band. The experimental $\gamma(x)$ for Rh_xPd_{1-x} is not uniformly enhanced over the calculated rigid-band $\gamma(x)$. The experimentally observed field and temperature dependences of the magnetic susceptibility for Pd are consistent with the calculated $N(E)$.

I. INTRODUCTION

In recent years there has been great interest in explaining the increasing tendency towards ferromagnetism and the simultaneous disappearance of superconductivity through the sequence of fcc 4d and 5d transition metals: Ir, Rh, Pt, and Pd.[1] Particular attention has been paid to the role of spin fluctuations,[2] produced by the strong exchange interactions among the d electrons. A starting point for the quantitative explanation of such effects is an accurate knowledge of the parameters of the one-electron theory for these metals,[3,4] and we have therefore calculated surfaces